

Anomalous magnetization reversal due to proximity effect of antiphase boundariesR. G. S. Sofin,^{*} Han-Chun Wu, and I. V. Shvets*CRANN, School of Physics, Trinity College Dublin, Dublin 2, Ireland*

(Received 9 May 2011; revised manuscript received 10 November 2011; published 8 December 2011)

Here we report anomalous double switching hysteresis loop and high coercivity (~ 0.1 T) in $\text{Fe}_3\text{O}_4(110)$ thin films. Our analytical model based on spin chains confined within small antiphase boundary domains (APBDs) suggests a significant proximity effect of antiferromagnetic antiphase boundaries (APBs). Furthermore, the calculated domain size (D) follows the well-known scaling relation $D = C\sqrt{t}$. The results suggest that the interface exchange coupling between neighboring magnetic domains through antiferromagnetic APBs is responsible for the double switching hysteresis. Our findings could help advance the studies of anomalous properties of magnetic materials originating from growth defects. This effect can be utilized for the tunability of exchange bias in devices.

DOI: [10.1103/PhysRevB.84.212403](https://doi.org/10.1103/PhysRevB.84.212403)

PACS number(s): 68.55.Ln, 75.70.Kw, 75.30.Gw

Anomalous magnetic properties of ferromagnets originating due to defect driven structural modifications have received much attention in application oriented research.¹⁻⁴ Antiphase boundaries (APB) are natural growth defects occurring due to the symmetry difference between the thin film and the substrate crystal structures.⁵⁻⁷ Studies of epitaxial thin films and heterostructures containing APBs have attracted considerable attention during the last decade as APBs can significantly alter the physical properties of thin films, which is advantageous for the development of spintronic devices.⁸⁻¹¹ One of the important epitaxial heterostructures for these studies is Fe_3O_4 thin films grown on MgO substrates. Since the Fe_3O_4 ($Fd\bar{3}m$) crystal structure is lower in symmetry than MgO ($Fm\bar{3}m$) there are several equivalent nucleation sites on the MgO surface, which enforce the formation of APBs at the junctions of neighboring grains. The APBs can be considered as the disruption of cation chains in a continuous oxygen lattice. In $\text{Fe}_3\text{O}_4/\text{MgO}$ hetero-epitaxy there exist many new exchange interactions across APBs which are not present in the bulk. The observation of magnetoresistance in Fe_3O_4 films is explained on the basis of spin polarized conduction across the antiferromagnetically (AF) coupled APBs.¹²⁻¹⁵ Our previous analysis showed that in $\text{Fe}_3\text{O}_4(110)/\text{MgO}(110)$ films, APBs can be formed with three different shift vectors (i.e., $\frac{1}{2}\mathbf{a}(001)$ along $\langle 001 \rangle$ and $\frac{\sqrt{3}}{2}\mathbf{a}\langle \bar{1}11 \rangle$ or $\frac{\sqrt{3}}{2}\mathbf{a}\langle \bar{1}\bar{1}\bar{1} \rangle$ along the $\langle \bar{1}10 \rangle$ direction¹⁶). The islands separated by these shift vectors form APBs when they coalesce. Figure 1(a) shows one such possible APB formation with the boundary along the $\langle \bar{1}10 \rangle$ direction. We can identify two important superexchanges across these APBs which are 180° Fe-O-Fe and Fe-O-O-Fe, both AF in nature.^{17,18} It is well known that the size of the domains (D) enclosed by APBs shrinks with a decrease in film thickness (t), following the scaling relation¹⁹ $D = C\sqrt{t}$. In this Brief Report, we report the observation of strong film thickness dependent double switching behaviour in $\text{Fe}_3\text{O}_4(110)/\text{MgO}(110)$ films. We demonstrate that the double switching behavior in these films is a result of the disruption of the exchange interaction in proximity to APBs, so that some areas in the film become antiferromagnetically exchange coupled with each other.

Fe_3O_4 films with thicknesses 20, 30, and 60 nm were grown on (110) oriented MgO single crystal substrates (cut along the [110] direction within 0.5°) using oxygen plasma

assisted molecular beam epitaxy (MBE) system (DCA MBE M600) with a base pressure 5×10^{-10} Torr. For growth conditions see Ref. 5. The structural characterization of the films was performed using a multocrystal high-resolution x-ray diffractometer (HRXRD, Bede-D1, Bede, UK). The \mathbf{a}_\perp values for the films, calculated from the separation of (220) and (440) symmetric Bragg reflections of MgO and Fe_3O_4 film, respectively, shows $8.3943\text{\AA}(\pm 10^{-4}\text{\AA})$ for 20 and 30 nm films and $8.3952\text{\AA}(\pm 10^{-4}\text{\AA})$ for a 60-nm film. From the analysis of the grazing exit and grazing incidence asymmetric scans we obtained the in-plane lattice parameter \mathbf{a}_\parallel of the films. The detailed structural characterization shows that the 60-nm film undergoes a 0.7% strain relaxation and 20- and 30-nm films are fully strained. No iron oxide phases were observed other than Fe_3O_4 . In previous reports we have shown that the Fe_3O_4 growth procedure, which we follow in this work, does not form any unreacted Fe clusters or other impurities such as Mg in the bulk or interface of the film.^{20,21} Resistivity was measured as a function of temperature for various thicknesses and all the films underwent Verwey transition at temperatures (T_v) around 108 K. Since T_v is very sensitive to the Fe_3O_4 film stoichiometry, the very presence of the Verwey transition confirms that the films are of high quality.^{22,23} Figure 2 shows hysteresis loops (HL) obtained at room temperature with the magnetic field aligned along $[\bar{1}10]$ (M is normalized with saturation magnetization M_s). The HLs show a double switching behavior with two switching fields H_{c1} and H_{c2} being strongly thickness dependent, while with the field along [001] they show a hard axis behavior. We would like to stress that the double switching HL presented here is representative and reproducible. All our (110) films with thickness less than 60 nm showed similar behavior. Although bulk magnetite has cubic anisotropy with $\langle 111 \rangle$ easy axis, reports on magnetization studies in $\text{Fe}_3\text{O}_4(110)$ epitaxial films grown on MgO (110) substrates, show a square hysteresis loop with an in-plane $\langle \bar{1}10 \rangle$ easy axis and hard axis along $\langle 001 \rangle$, which are broadly consistent with our measurements.²⁴

Before discussing the double switching behavior of the HL we will discuss the details of the spin rotation in a magnetic domain confined by two AF-APBs [shown in Figs. 1(c) and 1(d)] under external field (H). At a sufficient field all the spins far from the AF-APBs follow the direction of H and spins near to the AF-APBs gradually rotate toward 90° out

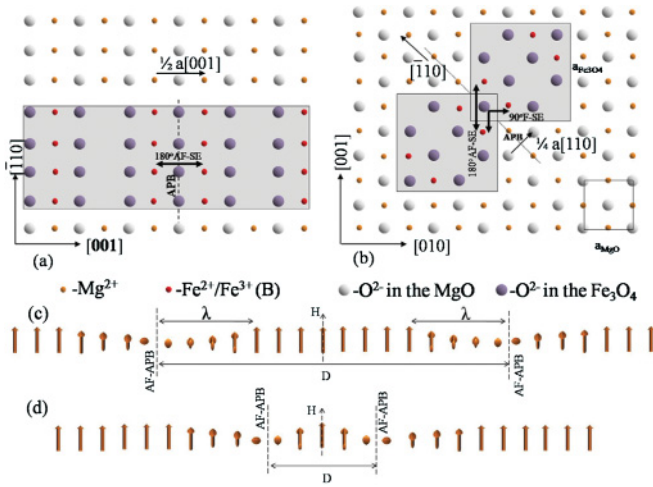


FIG. 1. (Color online) (a) Schematic of the APB formation in the $\text{Fe}_3\text{O}_4(110)/\text{MgO}(110)$ system and (b) APB formation in the $\text{Fe}_3\text{O}_4(100)/\text{MgO}(100)$ system. The figures represent what happens when two nucleation sites coalesce on the surface of the substrate. (c, d) Schematic representation of the dependence of θ on D in a field H .

of plane with respect to the field to facilitate AF coupling across the boundary. The Zeeman energy has to compete with the anisotropy energy and ferromagnetic exchange energy to align the spins toward the field direction. By considering the spin coherent rotation inside the domain, the angle between the spins θ is inversely proportional to D , the domain size. As D decreases with t , θ increases and a greater field is needed

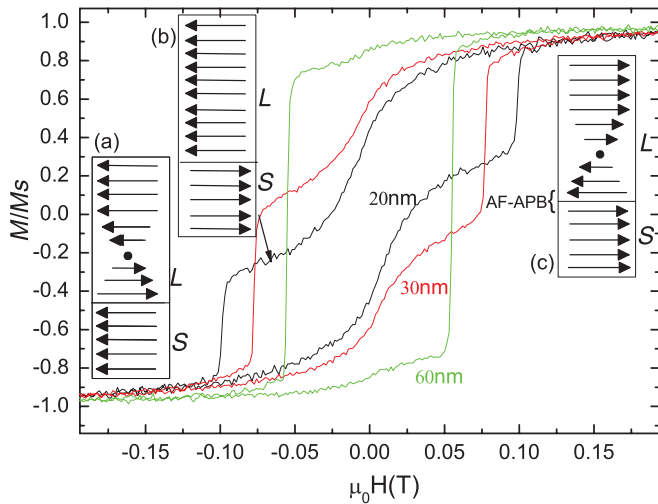


FIG. 2. (Color online) Normalized magnetization loops for 20-, 30-, and 60-nm films. Inset shows the possible spin configurations of a small (S) and a large (L) magnetic domains under interfacial exchange coupling. Insets (a) and (c) are the cases above the critical field where the magnetization in the small domains are pinned to the direction of the field (due to the competition between the AF coupling energy, with the ferromagnetic exchange, anisotropy, and Zeeman energies). To accommodate the AF coupling at the boundary the out-of-plane component of magnetization has to be in the large domain, which is due to the rotation of spins from antiparallel to parallel configuration with a small angle between the spins.

to compensate the anisotropy and exchange energy. Therefore, the critical field increases with decreasing film thickness.

To estimate the critical field we consider a model of a spin chain on one side of the AF-APB which is widely used for the analysis of magnetoresistance in Fe_3O_4 films.¹² In the present case the field is applied along the $[\bar{1}10]$ direction and the magnetocrystalline anisotropy energy density is also considered. This model is then modified to position a second AF-APB at a certain distance away from the first AF-APB. In this case we can write the energy per unit area of a chain as

$$\gamma_{001} = \int_{-\lambda}^0 \left[M_s H (1 - \cos\phi) + K \left(\frac{1}{4} \cos^2 2\phi \right) + A_F \left(\frac{d\phi}{dx} \right)^2 \right] dx, \quad (1)$$

where ϕ is the angle between local saturation magnetization M_s at distance x from the boundary and field H . λ is the distance from the APB at which the spins are approximately aligned along the field. The first term in the integral is the Zeeman energy density and the second term is the anisotropy energy density. The third term is the exchange energy density. K is the magnetocrystalline anisotropy constant and A_F is the exchange stiffness constant. With variational calculus the condition for minimum energy can be derived as

$$M_s H \sin\phi - K \cos 2\phi \sin 2\phi - 2A_F \left(\frac{d^2\phi}{dx^2} \right) = 0. \quad (2)$$

Multiplying by $\frac{d\phi}{dx}$ and integrating from 0 to λ with boundary conditions at $x = 0$, $\phi = \phi_0$, and at $x = -\lambda$ $\phi = 0$ we get

$$M_s H (1 - \cos\phi_0) - \frac{K}{8} (1 - \cos 4\phi_0) = A_F \left(\frac{d\phi}{dx} \right)^2. \quad (3)$$

Considering smaller domains, where the diameter $D \leq 2\lambda$, the factor $\frac{d\phi}{dx}$ will reduce by half due to the proximity effects of the adjacent APB. Therefore, dividing the right-hand side of Eq. (3) by a factor of 4 and further integrating, using the boundary conditions at $x = 0$, $\phi = \phi_0 = \frac{\pi}{2}$, and at $x = -\lambda$, $\phi = 0$, we can show that the critical field is given by

$$H_c = \frac{\pi^2 A_F}{8M_s \lambda^2}. \quad (4)$$

By using the value of H_{c2} , D (for which $D \approx 2\lambda$, the limiting distance at which the interaction of APBs starts) was calculated from Eq. (4) and was found to follow the well-known scaling relation $D = C\sqrt{t}$ (see Fig. 3). The slope $C = 2.35 \times 10^{-4} \text{ nm}^{0.5}$ obtained from Fig. 3 is similar to the one reported for (100) oriented films which is $C = 2.23 \times 10^{-4} \text{ nm}^{0.5}$ (Ref. 19). The domain sizes calculated for our (110) oriented films are found to be on average 9.7% smaller than the corresponding domain sizes reported in the case of (100) oriented films for the same film thickness.¹⁹ By considering that around 20–30% of APBs are AF-APBs^{11,25} and the mean domain size of our (110) oriented films is significantly smaller than in the case of (100) oriented films, we can consider the possibility of exchange coupling of neighboring magnetic domains through AF-APBs. For a greater understanding let us consider a simplified situation, where two magnetic domains of different size, large domain (L), and small domain (S)

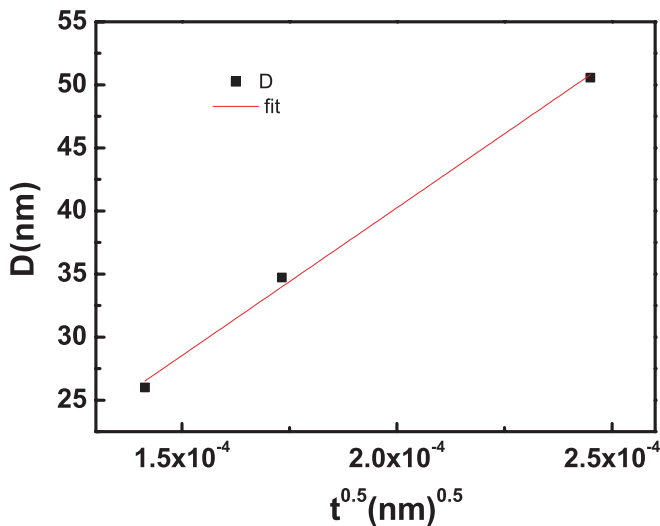


FIG. 3. (Color online) Variation of calculated domain size D with film thickness. The straight line represents a fit to the data using the scaling relation $D = C\sqrt{t}$.

are exchange coupled through the in-plane AF-APBs. It is clear that the AF-APBs induce an AF interfacial exchange coupling²⁶ which increases the critical field of small size domains and decreases the critical field of the large size domains causing the double switching in HLs. Please note that the AF exchange coupling in the referred paper is through an MgO barrier layer,²⁶ while, in our case, the AF exchange coupling is through AF-APBs. The spin configurations at different stages of the hysteresis loop are shown schematically in the inserts of Fig. 2. Our simple two-domain model can explain results for the low thickness sample well. However, when the film thickness is above 20 nm, the step in the magnetization decreases to a positive value. A possible reason could be the complexity of the domain distribution within the film, in particular the ratio between the number of small

domains and number of large domains due to the random distribution of AF-APB. Indeed, the APB density and their distributions are thickness dependent.¹⁹ We did not observe similar double HL in (100) oriented films grown on MgO (100) substrates. The reason could be the difference in the way Fe-O-Fe ions meet at the APBs in these two cases due to symmetry differences. For example, one such difference is depicted in Figs. 1(a) and 1(b). Here the APB formation along the $[\bar{1}10]$ direction on a (110) and (100) orientated MgO surface are compared. Figure 1(a) shows a perfect 180° AF super exchange while Fig. 1(b) shows the superposition of 180° AF as well as 90° ferromagnetic super exchanges. This superposition of two opposite types of exchange interaction in the latter case could reduce the AF coupling strength. We have not considered the energy density of AF coupling at the boundary $\gamma_{AF-APB} = \frac{A_{AF}}{d}(1 - \cos\phi_{AF})$ (where A_{AF} is the negative exchange stiffness constant for the AF exchange interaction at the boundary, d is the distance between the neighboring chains along the boundary, and ϕ_{AF} is the angle between the spins across boundary), in our analytical model. But the value of A_{AF} should have a prominent effect in the rotation of short spin chains since it dictates the rigidity of the spin chain near the boundary.

In conclusion we have shown that unusual hysteresis loops and large coercivity observed in Fe_3O_4 (110) films originate from the proximity effects of adjacent AF-APBs on shorter spin chains, which are confined within small APB domains. Our analytical model calculates the approximate APB domain size which follows the well-known scaling relation. Interfacial exchange coupling between magnetic domains across AF-APBs is also discussed. By changing the density of the APBs using suitable annealing conditions or using stepped substrate surfaces the effect can be tuned for device applications.

This work was supported by the SFI, Contract No. 06/IN.1/I91.

*sofins@tcd.ie

¹A. Alam, B. Kraczek, and D. D. Johnson, *Phys. Rev. B* **82**, 024435 (2010).

²H. Z. Guo, J. Burgess, E. Ada, S. Street, A. Gupta, M. N. Iliev, A. J. Kellock, C. Magen, M. Varela, and S. J. Pennycook, *Phys. Rev. B* **77**, 174423 (2008).

³I. Monot-Laffez, M. Dominiczak, F. Giovannelli, A. Ruyter, M. D. Rossell, and G. V. Tendeloo, *J. Appl. Phys.* **101**, 053502 (2007).

⁴Yi Ding, Yanli Wang, and Jun Ni, *J. Phys. Chem. C* **114**, 12416 (2010).

⁵M. Luysberg, R. G. S. Sofin, S. K. Arora, and I. V. Shvets, *Phys. Rev. B* **80**, 024111 (2009).

⁶A. V. Ramos, J.-B. Moussy, M.-J. Guittet, A. M. Bataille, M. Gautier-Soyer, M. Viret, C. Gatel, P. Bayle-Guillemaud, and E. Snoeck, *J. Appl. Phys.* **100**, 103902 (2006).

⁷J.-B. Moussy, S. Gota, A. Bataille, M.-J. Guittet, M. Gautier-Soyer, F. Delille, B. Dieny, F. Ott, T. D. Doan, P. Warin, P. Bayle-Guillemaud, C. Gatel, and E. Snoeck, *Phys. Rev. B* **70**, 174448 (2004).

⁸D. T. Margulies, F. T. Parker, M. L. Rudee, F. E. Spada, J. N. Chapman, P. R. Aitchison, and A. E. Berkowitz, *Phys. Rev. Lett.* **79**, 5162 (1997).

⁹S. Tiwari, D. M. Phase, and R. J. Choudhary, *Appl. Phys. Lett.* **93**, 234108 (2008).

¹⁰S. Lee, A. Fursina, J. T. Mayo, C. T. Yavuz, V. L. Colvin, R. G. S. Sofin, I. V. Shvets, and D. Natelson, *Nat. Mater.* **7**, 130 (2008).

¹¹H. C. Wu, M. Abid, B. S. Chun, R. Ramos, O. N. Mryasov, and I. V. Shvets, *Nano Lett.* **10**, 1132 (2010).

¹²W. Eerenstein, T. T. M. Palstra, S. S. Saxena, and T. Hibma, *Phys. Rev. Lett.* **88**, 247204 (2002).

¹³S. K. Arora, R. G. S. Sofin, and I. V. Shvets, *Phys. Rev. B* **72**, 134404 (2005).

¹⁴R. G. S. Sofin, S. K. Arora, and I. V. Shvets, *J. Appl. Phys.* **97**, 10D315 (2005).

¹⁵W. Eerenstein, T. T. M. Palstra, and T. Hibma, *Thin Solid Films* **400**, 90 (2001).

- ¹⁶R. G. S. Sofin, S. K. Arora, and I. V. Shvets, *Phys. Rev. B* **83**, 134436 (2011).
- ¹⁷J. B. Goodenough, *Magnetism and the Chemical Bond* (Wiley Interscience, New York, 1963).
- ¹⁸T. Kasama, R. E. Dunin-Borkowski, and W. Eerenstein, *Phys. Rev. B* **73**, 104432 (2006).
- ¹⁹W. Eerenstein, T. T. M. Palstra, T. Hibma, and S. Celotto, *Phys. Rev. B* **66**, 201101(R) (2002).
- ²⁰S. K. Arora, R. G. S. Sofin, I. V. Shvets, and M. Luysberg, *J. Appl. Phys.* **100**, 073908 (2006).
- ²¹S. K. Arora, Han-Chun Wu, R. J. Choudhary, I. V. Shvets, O. N. Mryasov, Hongzhi Yao, and W. Y. Ching, *Phys. Rev. B* **77**, 134443 (2008).
- ²²R. Aragon, D. J. Buttrey, J. P. Shepherd, and J. M. Honig, *Phys. Rev. B* **31**, 430 (1985).
- ²³J. Orna, P. A. Algarabel, L. Morellón, J. A. Pardo, J. M. de Teresa, R. López Antón, F. Bartolomé, L. M. García, J. Bartolomé, J. C. Cezar, and A. Wildes, *Phys. Rev. B* **81**, 144420 (2010).
- ²⁴Q. Pan, T. G. Pokhil, and B. M. Moskowitz, *J. Appl. Phys.* **91**, 5945 (2002).
- ²⁵A. M. Bataille, L. Ponson, S. Gota, L. Barbier, D. Bonamy, M. Gautier-Soyer, C. Gatel, and E. Snoeck, *Phys. Rev. B* **74**, 155438 (2006).
- ²⁶H. C. Wu, S. K. Arora, O. N. Mryasov, and I. V. Shvets, *Appl. Phys. Lett.* **92**, 182502 (2008).